UAB
Universitat Autònoma de Barcelona

Dipòsit digital de documents de la UAB

This is the **accepted version** of the journal article:

Cosco, Jan [et al.]. «The effect of residual palladium catalyst contamination on the photocatalytic hydrogen evolution activity of conjugated polymers». *Advanced Energy Materials*, Vol. 8, Num. 34 (December 2018), art. 1802181 DOI 10.1002/AENM.201802181

This version is available at https://ddd.uab.cat/record/338627

under the terms of the IN COPYRIGHT license.

WILEY-VCH

DOI: 10.1002/ ((please add manuscript number))
Article type: Full Paper

Title: The Effect of Residual Palladium Catalyst Contamination on the Photocatalytic Hydrogen Evolution Activity of Conjugated Polymers

Jan Kosco[*†], Michael Sachs,[‡] Robert Godin,[‡,¶] Mindaugas Kirkus,[†] Laia Francas,[‡] Matthew Bidwell,[‡] Muhammad Qureshi,[§] Dalaver Anjum,[§] James R Durrant,[‡] and Iain McCulloch[†‡]*

[†]Department of Physical Sciences and Engineering, KAUST Solar Centre (KSC), 4700 KAUST, Thuwal, Saudi Arabia. [‡]Department of Chemistry and Centre for Plastic Electronics, Imperial College London, South Kensington Campus, London SW7 2AZ, U.K. [§] Department of Physical Sciences and Engineering, KAUST Catalysis Centre (KCC), 4700 KAUST, Thuwal, Saudi Arabia. [¶]Present address: The University of British Columbia, Okanagan Campus, Department of Chemistry, 3247 University Way, Kelowna, BC, V1V V1Y, Canada

Keywords: photocatalysis, organic, hydrogen evolution, water splitting, polymers

The effect of residual Pd on hydrogen evolution activity in conjugated polymer photocatalytic systems was systematically investigated using colloidal poly(9,9-dioctylfluorene-alt-benzothiadiazole) (F8BT) nanoparticles as a model system. Residual Pd, originating from the synthesis of F8BT via Pd catalyzed polycondensation polymerization, was observed in the form of homogenously distributed Pd nanoparticles within the polymer. Residual Pd was essential for any hydrogen evolution to be observed from this polymer, and very low Pd concentrations (<40 ppm) were sufficient to have a significant effect on the hydrogen evolution reaction (HER) rate. The HER rate increased linearly with increasing Pd concentration from <1 ppm to approximately 100 ppm, at which point the rate began to saturate. Transient absorption spectroscopy experiments support these conclusions, and suggest that residual Pd mediates electron transfer from the F8BT nanoparticles to protons in the aqueous medium.

1. Introduction

In recent years there has been a growing interest in developing organic semiconductors capable of driving photocatalytic water splitting due to their low cost, aqueous stability, and tunable band gaps. Graphitic carbon nitrides remain the most well-known and intensely studied class of organic semiconductors for this application.[1–6] Recently however, new classes of materials are being investigated for hydrogen evolution from water, such as nitrogen doped graphene oxide,[7] covalent organic frameworks,[8–10] conjugated polymer networks,[11–14] and linear conjugated polymers.[15–20] With the notable exception of graphitic carbon nitride,[21] most organic semiconductors have required an additional metal co-catalyst to produce an appreciable H_2 evolution rate, often introduced by Pt photodeposition,[22] or the addition of a molecular catalyst.[8,23,24] However, recent reports of photocatalysis employing both linear and cross linked conjugated polymers suggest that these systems are able to produce H_2 under visible light irradiation without any added co-catalyst, at a much faster rate than commercial graphitic carbon nitride, even when the latter is subjected to Pt photodeposition.[11] Activity without the need for co-catalysts, which are often precious metals or molecular complexes with limited stability,[25] could be a very attractive feature of such polymer photocatalysts with the potential to vastly reduce the cost and complexity of current photocatalytic systems.

Comentat [Jk1]: Reviewer 1 comments 1-2, reviewer 3 comment 1. Suggested references added.

A feature of these linear and crosslinked conjugated polymers that has not yet been systematically studied is the presence of significant quantities of residual Pd originating from their synthesis via Pd catalysed polycondensation reactions.[11,12,15,26] It has previously been shown that the molecular Pd catalysts used in these reactions can decompose via deligation and subsequent Ostwald ripening to form metallic Pd^0 particles which are strongly retained within the polymer matrix and are difficult to remove via classical purification techniques.[27–31] Similarly to Pt^0, Pd^0 is a highly active proton reduction electrocatalyst.[32–34] Therefore, it is possible that the residual Pd, dispersed within these polymer structures, facilitates H_2

evolution and removes the need for additional co-catalysts. Much uncertainty remains about the nature of the active site in conjugated polymer systems, and there are conflicting views in the literature on whether or not the residual amounts of Pd play a significant role. No correlation was seen between Pd concentration and hydrogen evolution reaction (HER) rate in a range of conjugated microporous polymers,[11] and in a series of linear polymers containing the 2,1,3-benzothiadiazole (BT) unit, it was concluded that it was H-bonding from water to the N atoms on this unit that facilitated proton reduction, not residual Pd.[35] In the most in depth study to date, a dependency of HER rate on Pd content was observed when Pd catalyst loadings were altered during the synthesis of a conjugated polymer network.[12] However, altering catalyst loadings changed the degree of polymerisation of the polymer, and may have also altered the network's microstructure. Consequently, it was impossible to completely decouple the effects these structural changes may have had on HER rate from the effect of residual Pd. Furthermore, due to the crosslinked structure of the polymer it was not possible to reduce the Pd mass concentration below 400 ppm (0.04 wt.%). Therefore, it could not be determined whether these conjugated polymers could drive the HER without Pd, or Pd only accelerated the HER rate, similarly to Pt in carbon nitrides.[36,37] The question whether such conjugated polymer systems are intrinsically able to photocatalytically reduce protons to H_2 or require a co-catalyst such as Pd to drive this reaction is therefore of great interest.

In this work, the role of residual Pd in conjugated polymer photocatalytic systems was systematically investigated using poly(9,9-dioctylfluorene-alt-benzothiadiazole) (F8BT) as a model system. F8BT was chosen as a model polymer due to energy levels suitable for proton reduction and visible light absorption,[38] and its solubility which allows purification post polymerization. The Pd mass concentration in F8BT was altered post polymerization between <1 ppm and 1170 ppm using purification methods that did not alter the polymer's molecular structure (**Figure S1**). Transmission electron microscopy (TEM) revealed that Pd was present

in the polymer in the form of homogenously distributed nanoparticles with an average diameter of 3.2 nm. F8BT was then processed into colloidal nanoparticles using a modified nanoprecipitation method,[39] and the HER activity of the nanoparticle suspensions was measured in the presence of diethylamine (DEA) as a sacrificial electron donor. It was found that increasing Pd concentration not only accelerated the HER rate, but that the presence of Pd was essential for any H_2 evolution to be observed. Transient absorption spectroscopy (TAS) experiments showed that long-lived electrons increasingly accumulate on the polymer as the Pd content is reduced, indicating that electron transfer to protons in the aqueous phase is impeded. The results presented herein show that residual Pd plays an essential role in the HER of F8BT nanoparticles, with implications for the function of other conjugated polymer photocatalytic systems.

2. Results and Discussion

F8BT was synthesized via Suzuki polymerization according to a literature procedure,[40] using tris(dibenzylideneacetone)dipalladium(0) (Pd2(dba)3) as the Pd catalyst (**Figure1**).

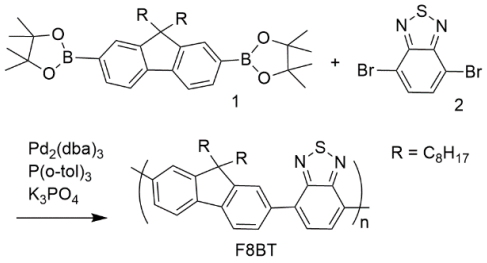
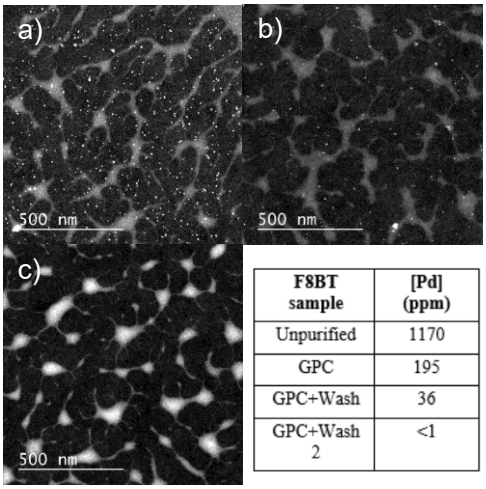


Figure 1. Structure and synthesis of F8BT from its monomers via Suzuki polymerization.

After initial sequential purification by Soxhlet extraction using methanol, acetone, and n-hexane solvents, over 1000 ppm (0.1 wt.%) of Pd remained inside the polymer. F8BT was then further purified by gel permeation chromatography (GPC), and washed two further times

with sodium diethyldithiocarbamate, a ligand shown to chelate and remove residual palladium.[28,41,42] A portion of polymer was retained after each purification stage, and the Pd concentration was measured by inductively coupled plasma optical emission spectrometry (ICP-OES). Purification resulted in a gradual decrease of Pd concentration to below the instrument's 1 ppm detection limit (**Inset, Figure 2**).



F8BT sample	[Pd] (ppm)
Unpurified	1170
GPC	195
GPC+Wash	36
GPC+Wash 2	<1

Figure 2. Dark field TEM images of **a)** Unpurified **b)** GPC **c)** GPC + Wash 2 F8BT films showing the decreasing concentration of Pd nanoparticles. Inset: Table showing the Pd concentration in F8BT after each purification stage, as measured by ICP-OES.

TEM was used to image films of F8BT fractions before and after purification in order to verify the presence of Pd nanoparticles within the films, and to confirm that the purification procedures were successful in removing them (**Figure 2**). The TEM images reveal that unpurified F8BT contained a large number of dense nanoparticles (445 particles in 1 μm^2, average diameter 4.6 nm) which dramatically decreased upon GPC purification (137 particles in 1 μm^2, average diameter 4.0 nm). No particles were observed in the sodium diethyldithiocarbamate washed F8BT. Taking into account the approximate particle volume, these observations are consistent with the ICP-OES measured Pd concentrations, and suggest

that the dense nanoparticles are formed of Pd which can be removed by the successive purification steps employed.

Following purification, F8BT samples containing varying levels of Pd were blended with poly(styrene-co-maleic anhydride) (PSMA) and processed into nanoparticles via nanoprecipitation (see experimental section in SI). PSMA was used as a stabiliser to prevent F8BT nanoparticle aggregation. Several additional samples were also prepared with specifically tailored Pd concentrations by adding $Pd_2(dba)_3$ to completely purified F8BT (<1 ppm Pd) before nanoprecipitation. Nanoparticle size distributions were measured by dynamic light scattering (DLS, **Figure 3, Table 1**) which revealed that each nanoparticle batch had a unimodal size distribution, and that the average nanoparticle diameter between batches was relatively constant at approximately 50 nm. This is important when comparing HER rates between batches, because nanoparticle size affects the total surface area available for reaction, which would likely affect HER rate.

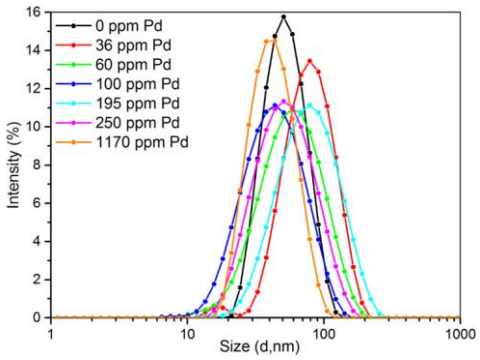


Figure 3. Nanoparticle size distributions by intensity, measured by DLS. Histograms have been plotted as frequency polygons for greater clarity.

Table 1. Summary of DLS nanoparticle size distribution data.

Pd concentration [ppm]	Z-average diameter [nm]	Polydispersity index
<1	49.6	0.101
36	55.2	0.160
60	54.0	0.190
100	43.1	0.212
195	68.0	0.186
250	46.4	0.178
1170	40.1	0.118

Having samples of the same size eliminates this effect and allows the effect of Pd concentration to be isolated. Imaging of the nanoparticle samples by Cryo-TEM (**Figure 4**) revealed that the F8BT/PSMA blends precipitated as globular particles, with sizes ranging between approximately 30 and 70 nm, which is in good agreement with the DLS size distributions.

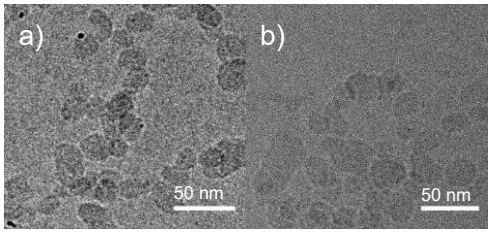


Figure 4. Bright field Cryo-TEM images of F8BT nanoparticle suspensions formed from **a)** unpurified, and **b)** GPC + Wash 2 F8BT.

Furthermore, it can be seen that many polymer particles contain one or more smaller, dense particles with a diameter of approximately 1-5 nm (**Figure 4a**). These are approximately the same size as those seen within the F8BT films before nanoprecipitation, and are attributed to Pd nanoparticles formed spontaneously from deligated $Pd_2(dba)_3$, similar to those found in

other polymers formed via Pd catalyzed polymerization.[28,43] The Pd nanoparticles are also present at the surface of some of the polymer particles and are therefore optimally placed to act as a catalytic interface between the polymer and protons in the surrounding water.

The HER activities of the nanoparticle suspensions were measured in the presence of DEA as a sacrificial electron donor under visible light irradiation (385-700 nm) from a 300 W Xe lamp (irradiance spectrum shown in **Figure S8**) over 24 hours. **Figure 5** shows that the photocatalytic performance of the F8BT nanoparticles is highly dependent on the concentration of Pd in the polymer.

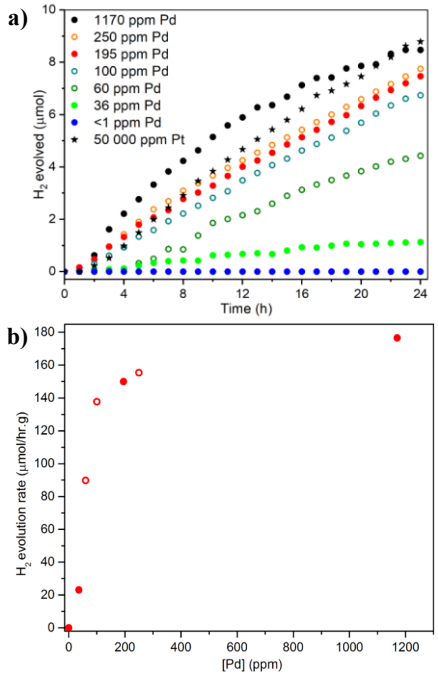


Figure 5. a) H_2 evolution from F8BT nanoparticles containing varying amounts of Pt or Pd. Full circles represent samples containing residual Pd. Hollow circles represent samples in which $Pd_2(dba)_3$ was added back into GPC + Wash 2 F8BT. Stars represent pristine F8BT nanoparticles subjected to Pt photodeposition. **b)** Average H_2 evolution rate over 24 h from

colloidal F8BT nanoparticles as a function of Pd concentration. H_2 evolution measurements were performed on 2 mg of F8BT in 3:7 DEA:water (15 mL) under illumination from a 300 W Xe lamp (385-700 nm).

Comentat [Jk2]: Reviewer 3 comment 3

Nanoparticles formed from F8BT containing 1170 ppm residual Pd displayed an average HER rate of 176.6 µmol/h.g (EQE = 0.02% @ 340 nm), producing 8.47 µmol H_2 over 24 h. This HER rate is similar to several reported conjugated polymer photocatalytic systems,[11,20] however, robust performance comparisons between photocatalysts are difficult to make due to differing reactor setups and sacrificial reagents used. Nanoparticles formed from F8BT containing <1 ppm residual Pd were completely inactive, producing <0.02 µmol H_2 (below the GC detection limit) over the same time period. This shows that Pd is an essential component of the F8BT nanoparticles without which no HER activity is observed. To the best of our knowledge, this is the first report which shows that removing all of the residual Pd from a polymer synthesized by Pd catalyzed cross coupling polymerization results in a complete loss of photocatalytic activity.

Comentat [Jk3]: Reviewer 1 comment 3

To confirm that the performance decrease after polymer purification was indeed due to the decrease in Pd concentration and not due to the removal of other contaminants or degradation of the polymer, measurements (hollow circles) were taken with samples which were prepared by controlled additions of Pd to the pristine polymer in the form of $Pd_2(dba)_3$ (see experimental section). Once Pd was reintroduced into the polymer (**Figure S10**), the HER activity was recovered proportionally to Pd concentration, which confirmed that Pd was the species that facilitated H_2 evolution.

For further insights into the influence of residual Pd on the photophysics of our F8BT nanoparticles we performed transient absorption spectroscopy (TAS) measurements. As shown in **Figure 6**, experiments on µs – ms time scales reveal the emergence of a long-lived

excited state absorption in the presence of DEA which extends throughout the visible and near-infrared spectral range and is characterized by an increasing amplitude towards 500 nm.

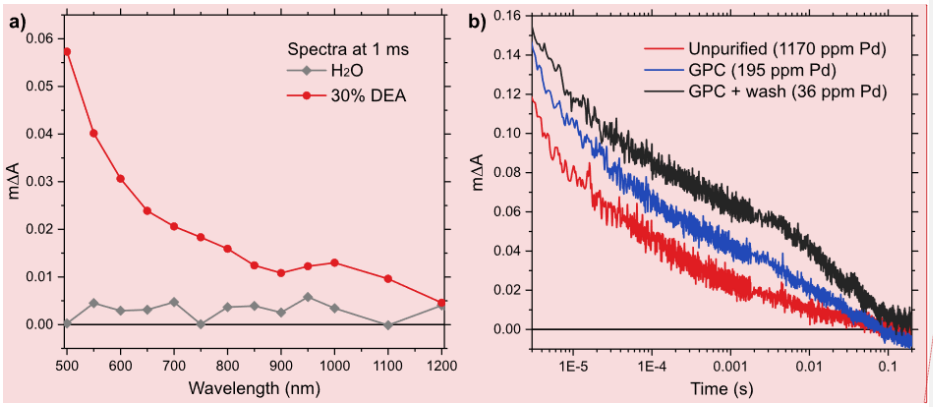


Figure 6. Transient absorption measurements of F8BT nanoparticle suspensions. **a)** Transient spectrum of unpurified F8BT (1170 ppm Pd) at 1 ms, both in pure H_2O and in an aqueous suspension containing 30% DEA. **b)** Transient kinetics probed at 750 nm for different Pd concentrations in an aqueous suspension containing 30% DEA. All data were obtained at an excitation wavelength of 460 nm and a fluence of 0.54 mJ cm^{-2}. Suspensions were prepared with an absorbance of 0.42 at 460 nm and carefully purged with argon before the experiment.

This long-lived signal only appears upon addition of the electron donor DEA (**Figure 6a**) and is quenched significantly in the presence of oxygen (**Figure S11**), which, taken together, suggests that this long-lived signal can be assigned to photogenerated electrons on the F8BT polymer (electron polarons). This assignment is in line with the observation of long-lived electrons in carbon nitride systems upon addition of hole scavengers.[44,45] Since previous studies have reported a transient spectrum with a maximum between 600 nm and 800 nm for F8BT polarons,[46,47] we attribute the different spectrum observed here primarily to the aqueous environment in our suspension systems.

To investigate the dependence of the long-lived electron signal upon Pd concentration, we probed the transient kinetics in F8BT nanoparticle suspensions with different levels of purification. Kinetics at 750 nm were chosen to avoid the photoluminescence artefacts (photoluminescence maximum λ_{PL} = 550 nm) that are present at early times for shorter probe

Comentat [Jk4]: Reviewer 3 comment 7

wavelengths. As shown in **Figure 6b**, we observe an increasing signal amplitude with decreasing Pd content, with the relative differences becoming increasingly large at longer timescales (the Unpurified sample has signal 1.2x smaller at 3 µs and 4x smaller at 10 ms compared to the GPC + wash sample). We attribute this increasing signal amplitude to an increased accumulation of long lived photogenerated F8BT electrons in the absence of Pd, consistent with the presence of Pd accelerating photocatalytic hydrogen generation and therefore suppressing the accumulation of long lived electrons. This suppression of long lived electrons in the presence of metal catalyst, correlated with increased hydrogen generation is analogous to results we have reported previously for carbon nitride photocatalysts with Pt and molecular nickel based proton reduction co-catalysts,[45] and supports the key role of Pd in catalyzing proton reduction in the F8BT nanoparticles studied herein. As Pd is a highly active hydrogen evolution electrocatalyst,[32,33] it is likely that the nanoparticles of residual Pd embedded within the surface of the F8BT nanoparticles act as a co-catalyst; similarly to photodeposited Pt on graphitic carbon nitride[36,37] or TiO_2[48]. This assignment is in line with the observed linear increase of the HER rate with Pd mass concentrations between 0 and approximately 100 ppm Pd. Higher Pd concentrations produce a sub-linear rate increase, with very little rate enhancement between 250 and 1170 ppm Pd. This saturation of performance is typical of the transition between a kinetically limited and a mass transport limited reaction rate,[49,50] suggesting that at low Pd concentrations the HER rate is limited by the availability of Pd based active sites. As the concentration of Pd increases, these become more abundant, and the HER rate becomes limited by factors affecting the efficiency of transport of either electrons or protons to these active sites, such as the efficiency of hole quenching by DEA. Interestingly, a very low Pd concentration (approximately 200 ppm) is sufficient to begin saturating the performance of the F8BT nanoparticles, and even photodeposition of 50,000 ppm (5 wt.%) Pt, a more efficient HER catalyst, does not produce a significant rate increase compared to 200 ppm Pd (stars, **Figure 5a**). The low Pd saturation concentration explains

Comentat [Jk5]: Reviewer 3 comment 6

why in similar systems reported in the literature there was no observed trend between Pd concentration and HER rate,[11] because in these systems the Pd concentration was on the order of 5000 ppm (0.5 wt.%); more than 20 times greater than the 200 ppm saturation limit shown for the F8BT system.

3. Conclusion

In conclusion, it was shown that F8BT synthesized via a standard Pd catalyzed polycondensation polymerization and purified by Soxhlet extraction contained over 1000 ppm (0.1 wt.%) of residual Pd. Subjecting the F8BT to a sequence of further purification steps gradually reduced the Pd concentration within the polymer to below 1 ppm without altering the polymer structure. The Pd was homogenously distributed within the polymer in the form of nanoparticles. When the bulk polymer was processed into nanoparticles, residual Pd remained in the particles, often on the polymer particle surface. Measuring the photocatalytic HER rate of the F8BT nanoparticle suspensions containing various Pd concentrations in the presence of DEA revealed that the Pd concentration had a profound effect on the HER rate. F8BT nanoparticles containing 1170 ppm Pd displayed an average HER rate of 176.6 μmol/h.g (EQE = 0.02% @ 340 nm), producing 8.47 μmol H_2 over 24 h . However, when all of the residual Pd was removed from the polymer, the particles became completely inactive, indicating acted as a co-catalyst for the HER. This assertion is supported by TAS measurements, which show that photogenerated electrons increasingly accumulate at lower Pd concentrations in the presence of DEA. These results demonstrate that residual Pd plays a significant role in the hydrogen evolution activity of organic semiconductor photocatalytic systems, even at ppm level concentrations. The presence of residual Pd should therefore be considered when designing organic systems for water splitting, as well as processes such as CO_2 reduction, where proton reduction is a competing and unwanted side reaction.

4. Experimental Section

Materials and methods

All chemicals were purchased from Sigma Aldrich and used without purification unless otherwise stated. Polymer purification by gel permeation chromatography (GPC) was carried out on a Shimadzu LC-20AD liquid chromatograph equipped with two Agilent PLgel 10 µm mixed-d columns. Polymer samples were digested using an UltraWAVE single reaction chamber microwave digestion system. Pd concentrations were measured by inductively coupled plasma optical emission spectrometry (ICP-OES, Agilent 5110). Sonication was carried out in an ultrasonic bath (Branson 5510). Nanoparticle size was measured by dynamic light scattering (DLS, Malvern Zetasizer ZS). TEM and Cryo-TEM images were taken using FEI Titan and Titan Krios transmission electron microscopes respectively.

F8BT synthesis

F8BT was synthesised from its monomers using a modified literature procedure.[40] Monomers were recrystallized from ethanol, and thoroughly dried prior to use. All solvents were thoroughly degassed with nitrogen prior to use. A solution of potassium phosphate (0.529 g, 2.49 mmol) in 2 mL water and 0.5 mL dioxane was added to a mixture of 9,9-Dioctyl-9H-fluorene-2,7-diboronic acid bis(pinacol) ester (**1**) (400 mg, 0.623 mmol), 4,7-Dibromobenzo[c]-1,2,5-thiadiazole (183 mg, 0.623 mmol), Tris(dibenzylideneacetone)dipalladium(0) ($Pd_2(dba)_3$) (5.7 mg, 6.22 µmol, 2 mol% Pd), and tri(o-tolyl)phosphine ($P(o\text{-}tol)_3$), (11.4 mg, 37.5 µmol, 6 mol%) in toluene (2 mL). The mixture was stirred vigorously inside a sealed microwave vial for 24 h at 110 ºC. The contents were removed, and washed by consecutive Soxhlet extractions with methanol, acetone, and hexane, each for 24 h. The polymer was extracted with chloroform, concentrated under reduced pressure, and precipitated into methanol. The yellow precipitate was filtered to obtain "unpurified" F8BT (Mn = 39.6 kD Mw = 84.4 kD, PDI = 2.13, 507 mg 87% yield).

FBT purification by gel permeation chromatography (GPC)

"Crude" F8BT (400 mg) was purified by gel permeation chromatography at 80ºC, using a 2 mL/min isocratic flow of chlorobenzene. The eluent was collected in fractions, and the central 75% fractions were kept, combined, and the solvent was removed under reduced pressure. The polymer was dissolved in a small amount of chloroform, precipitated into methanol, and filtered to obtain purified "GPC" F8BT (320 mg).

FBT purification by diethyldithiocarbamate wash

"GPC" F8BT (150 mg) was dissolved in chloroform (50 mL) and added to a solution of sodium diethyldithiocarbamate trihydrate (0.60 g, 2.35 mmol) in water (60 mL). The biphasic mixture was stirred vigorously at 60 ºC for 12 h under nitrogen. The chloroform phase was separated, and thoroughly washed with water (5 × 20 mL). The solution was concentrated under reduced pressure, precipitated into methanol, and filtered to obtain the purified "GPC + Wash" F8BT (141 mg). 80 mg of "GPC + Wash" F8BT was purified again following the same procedure to give 53 mg of "GPC + Wash 2" F8BT.

Measurement of residual palladium in polymers

The polymer sample was digested in a microwave digester (UltraWAVE) in a mixture of aqua regia containing a small amount of hydrogen peroxide and sulfuric acid. The digested sample was analysed by ICP-OES to determine the concentration of palladium in the sample.

Addition of Pd to purified F8BT

To add a specific concentration of Pd back into "GPC + wash 2" FBT (0 ppm residual Pd), an aliquot of $Pd_2(dba)_3$ solution was added to a solution of "GPC + wash 2" F8BT. For example, to add 100 ppm Pd back into "GPC + wash 2" F8BT, 25.0 µL of $Pd_2(dba)_3$ solution (10 ppm in THF) was added to 5.0 mL of "GPC + wash 2" F8BT (500 ppm in THF). The solution was heated in a sealed vial at 60 ºC overnight, and the solvent was removed. During this time the $Pd_2(dba)_{3\ \text{decomposed}}$ to Pd^0 nanoparticles and became fully mixed into the polymer (**Figure S10**). The dried polymer was then used to make nanoparticles as described below.

Nanoparticle preparation

Polymer nanoparticles were fabricated by nanoprecipitation using a method similar to one reported previously.[39] In a typical preparation, a solution of F8BT (500 ppm) and polystyrene-co-maleic anhydride (100 ppm) in tetrahydrofuran (5 mL) was filtered (0.2 µm PTFE syringe filter), then rapidly injected into MilliQ water (40 mL) under sonication in an ultrasonic bath. The mixture was sonicated for a further 2 min, and then heated in an oil bath at 80 ºC under constant nitrogen bubbling to remove the THF and concentrate the solution to 10 mL. Finally, the concentrated solution was filtered (0.45 µm glass fibre syringe filter) to remove large agglomerates. If stored in the dark, nanoparticle suspensions formed in this way were stable for several months without any signs of aggregation.

Hydrogen evolution measurements

Hydrogen evolution from colloidal F8BT nanoparticles was measured using DEA as a sacrificial electron donor. F8BT nanoparticles (2 mg) in 3:7 DEA:water (15 mL) were loaded into a recirculating batch reactor (area = 452 mm^2) which has been previously reported.[51] A starting pressure of 100 Torr was used. The suspension was illuminated with a 300 W Xe lamp (385-700 nm) and H_2 evolution was quantified by a gas chromatograph equipped with a thermal conductivity detector. EQE measurements were carried out in the same way, but with suitable band pass filters fitted to the light source.

Transient absorption measurements

Transient absorption measurements were conducted using a home-built transient absorption setup with a Nd:YAG laser (OPOTEK Opolette 355 II, 4 – 7 ns pulse width), which uses an optical parametric oscillator to generate 460 nm excitation pulses. These laser pulses are directed to the sample using a liquid light guide. A pyroelectric energy sensor (Ophir Photonics PE9) was used to measure excitation densities, here 0.54 mJ cm^{-2} at 460 nm. The output of a 100 W quartz halogen lamp (Bentham IL1) is used as a probe beam, with monochromators to select the probe wavelength positioned before and after the sample, and detected by a Si photodiode (Hamamatsu S3071). Appropriate long pass filters were placed between sample and detector and scattered laser light was used to start the data acquisition (Thorlabs DET210). Home-built LabVIEW-based software was used to record data: the detector output was amplified (Costronics 1999 amplifier) and sampled on the µs – ms timescale using an oscilloscope (Tektronix DPO 2012B), and the non-amplified signal was recorded on the ms timescale using a DAQ card (National Instruments, NI USB6211). The recorded data was processed in MATLAB and OriginPro 2017.

Supporting Information

Supporting Information is available from the Wiley Online Library or from the author.

Acknowledgements

We acknowledge funding from KAUST and BASF, as well as EPSRC Project EP/G037515/1, EP/M005143/1, EC FP7 Project SC2 (610115), and EC H2020 Project SOLEDLIGHT (643791). J.R.D. acknowledges support from ERC AdG Intersolar (291482) and M.S. thanks the Imperial College President's PhD Scholarship scheme. R.G. is grateful to FRQNT for a postdoctoral award. L.F. thanks the EU for a Marie Curie fellowship (658270).

Received: ((will be filled in by the editorial staff))
Revised: ((will be filled in by the editorial staff))
Published online: ((will be filled in by the editorial staff))

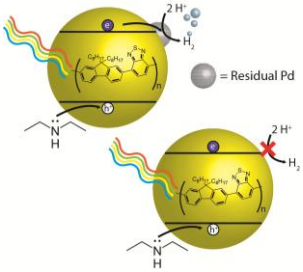
388 References

389 [1] A. Thomas, A. Fischer, F. Goettmann, M. Antonietti, J.-O. Müller, R. Schlögl, J. M.
390 Carlsson, *J. Mater. Chem.* **2008**, *18*, 4893.
391 [2] Y. Zheng, L. Lin, B. Wang, X. Wang, *Angew. Chemie Int. Ed.* **2015**, *54*, 12868.
392 [3] M.-Y. Ye, Z.-H. Zhao, Z.-F. Hu, L.-Q. Liu, H.-M. Ji, Z.-R. Shen, T.-Y. Ma, *Angew.*
393 *Chemie Int. Ed.* **2017**, *56*, 8407.
394 [4] S. Yang, Y. Gong, J. Zhang, L. Zhan, L. Ma, Z. Fang, R. Vajtai, X. Wang, P. M.
395 Ajayan, *Adv. Mater.* **2013**, *25*, 2452.
396 [5] X. Wang, K. Maeda, X. Chen, K. Takanabe, K. Domen, Y. Hou, X. Fu, M. Antonietti,
397 *J. Am. Chem. Soc.* **2009**, *131*, 1680.
398 [6] L. Zhang, J. Xiao, H. Wang, M. Shao, *ACS Catal.* **2017**, *7*, 7855.
399 [7] T.-F. Yeh, C.-Y. Teng, S.-J. Chen, H. Teng, *Adv. Mater.* **2014**, *26*, 3297.
400 [8] T. Banerjee, K. Gottschling, G. Savasci, C. Ochsenfeld, B. V. Lotsch, *ACS Energy Lett.*
401 **2018**, *3*, 400.
402 [9] X. Jiang, P. Wang, J. Zhao, *J. Mater. Chem. A* **2015**, *3*, 7750.
403 [10] V. S. Vyas, F. Haase, L. Stegbauer, G. Savasci, F. Podjaski, C. Ochsenfeld, B. V.
404 Lotsch, *Nat. Commun.* **2015**, *6*, 8508.
405 [11] R. S. Sprick, J. X. Jiang, B. Bonillo, S. Ren, T. Ratvijitvech, P. Guiglion, M. A.
406 Zwijnenburg, D. J. Adams, A. I. Cooper, *J. Am. Chem. Soc.* **2015**, *137*, 3265.
407 [12] L. Li, Z. Cai, Q. Wu, W.-Y. Lo, N. Zhang, L. X. Chen, L. Yu, *J. Am. Chem. Soc.* **2016**,
408 *138*, 7681.
409 [13] S. Ghasimi, S. Prescher, Z. J. Wang, K. Landfester, J. Yuan, K. A. I. Zhang, *Angew.*
410 *Chemie - Int. Ed.* **2015**, *54*, 14549.
411 [14] Z. J. Wang, S. Ghasimi, K. Landfester, K. A. I. Zhang, *Adv. Mater.* **2015**, *27*, 6265.
412 [15] D. J. Woods, R. S. Sprick, C. L. Smith, A. J. Cowan, A. I. Cooper, *Adv. Energy Mater.*
413 **2017**, 1700479.
414 [16] L. Li, R. G. Hadt, S. Yao, W.-Y. Lo, Z. Cai, Q. Wu, B. Pandit, L. X. Chen, L. Yu,
415 *Chem. Mater.* **2016**, *28*, 5394.
416 [17] L. Wang, R. Fernández-Terán, L. Zhang, D. L. A. Fernandes, L. Tian, H. Chen, H.
417 Tian, *Angew. Chemie* **2016**, *128*, 12494.
418 [18] S. Yanagida, A. Kabumoto, K. Mizumoto, C. Pac, K. Yoshino, *J. Chem. Soc. Chem.*
419 *Commun.* **1985**, *0*, 474.
420 [19] T. Shibata, A. Kabumoto, T. Shiragami, O. Ishitani, C. Pac, S. Yanagida, *J. Phys.*
421 *Chem.* **1990**, *94*, 2068.
422 [20] R. S. Sprick, B. Bonillo, R. Clowes, P. Guiglion, N. J. Brownbill, B. J. Slater, F. Blanc,
423 M. A. Zwijnenburg, D. J. Adams, A. I. Cooper, *Angew. Chemie Int. Ed.* **2016**, *55*, 1792.
424 [21] X. Wang, K. Maeda, A. Thomas, K. Takanabe, G. Xin, J. M. Carlsson, K. Domen, M.
425 Antonietti, *Nat. Mater.* **2009**, *8*, 76.
426 [22] K. Wenderich, G. Mul, *Chem. Rev.* **2016**, *116*, 14587.
427 [23] S. Chu, Y. Wang, C. Wang, J. Yang, Z. Zou, *Int. J. Hydrogen Energy* **2013**, *38*, 10768.
428 [24] S. Chu, Y. Wang, Y. Guo, P. Zhou, H. Yu, L. Luo, F. Kong, Z. Zou, *J. Mater. Chem.*
429 **2012**, *22*, 15519.
430 [25] J. R. McKone, S. C. Marinescu, B. S. Brunschwig, J. R. Winkler, H. B. Gray, *Chem.*
431 *Sci.* **2014**, *5*, 865.
432 [26] F. Wang, J. Mielby, F. H. Richter, G. Wang, G. Prieto, T. Kasama, C. Weidenthaler,
433 H.-J. Bongard, S. Kegnaes, A. Fürstner, F. Schüth, *Angew. Chemie Int. Ed.* **2014**, *53*,
434 8645.
435 [27] F. C. Krebs, R. B. Nyberg, M. Jørgensen, *Chem. Mater.* **2004**, *16*, 1313.
436 [28] K. T. Nielsen, K. Bechgaard, F. C. Krebs, *Macromolecules* **2005**, *38*, 658.
437 [29] D. Pun, T. Diao, S. S. Stahl, *J. Am. Chem. Soc.* **2013**, *135*, 8213.

[30] Z. Lu, S. S. Stahl, *Org. Lett.* **2012**, *14*, 1234.
[31] T. Xue, Z. Lin, C.-Y. Chiu, Y. Li, L. Ruan, G. Wang, Z. Zhao, C. Lee, X. Duan, Y. Huang, *Sci. Adv.* **2017**, *3*, e1600615.
[32] Y. Zheng, Y. Jiao, M. Jaroniec, S. Z. Qiao, *Angew. Chemie Int. Ed.* **2015**, *54*, 52.
[33] J. Hu, C. Zhang, X. Meng, H. Lin, C. Hu, X. Long, S. Yang, *J. Mater. Chem. A* **2017**, *5*, 5995.
[34] J. Zheng, W. Sheng, Z. Zhuang, B. Xu, Y. Yan, *Sci. Adv.* **2016**, *2*, e1501602.
[35] P. B. Pati, G. Damas, L. Tian, D. L. A. Fernandes, L. Zhang, I. B. Pehlivan, T. Edvinsson, C. M. Araujo, H. Tian, *Energy Environ. Sci.* **2017**, *10*, 1372.
[36] Y. Shiraishi, Y. Kofuji, S. Kanazawa, H. Sakamoto, S. Ichikawa, S. Tanaka, T. Hirai, *Chem. Commun.* **2014**, *50*, 15255.
[37] J. Liu, Y. Zhang, L. Lu, G. Wu, W. Chen, *Chem. Commun.* **2012**, *48*, 8826.
[38] L. Wang, R. Fernández-Terán, L. Zhang, D. L. A. Fernandes, L. Tian, H. Chen, H. Tian, *Angew. Chemie Int. Ed.* **2016**, *55*, 12306.
[39] C. Wu, Y. Jin, T. Schneider, D. R. Burnham, P. B. Smith, D. T. Chiu, *Angew. Chemie Int. Ed.* **2010**, *49*, 9436.
[40] W. Zhang, J. Smith, R. Hamilton, M. Heeney, J. Kirkpatrick, K. Song, S. E. Watkins, T. Anthopoulos, I. McCulloch, *J. Am. Chem. Soc.* **2009**, *131*, 10814.
[41] B. C. Schroeder, S. Rossbauer, R. J. Kline, L. Biniek, S. E. Watkins, T. D. Anthopoulos, I. McCulloch, C. B. Nielsen, *Macromolecules* **2014**, *47*, 2883.
[42] V. W. Rosso, *Org. Process Res. Dev.* **1997**, *1*, 311.
[43] C. Bracher, H. Yi, N. W. Scarratt, R. Masters, A. J. Pearson, C. Rodenburg, A. Iraqi, D. G. Lidzey, *Org. Electron.* **2015**, *27*, 266.
[44] R. Godin, Y. Wang, M. A. Zwijnenburg, J. Tang, J. R. Durrant, *J. Am. Chem. Soc.* **2017**, *139*, 5216.
[45] H. Kasap, C. A. Caputo, B. C. M. Martindale, R. Godin, V. W. Lau, B. V. Lotsch, J. R. Durrant, E. Reisner, *J. Am. Chem. Soc.* **2016**, *138*, 9183.
[46] M. A. Stevens, C. Silva, D. M. Russell, R. H. Friend, *Phys. Rev. B* **2001**, *63*, 165213.
[47] M. J. Bird, J. Bakalis, S. Asaoka, H. Sirringhaus, J. R. Miller, *J. Phys. Chem. C* **2017**, *121*, 15597.
[48] Z. Jiang, Z. Zhang, W. Shangguan, M. A. Isaacs, L. J. Durndell, C. M. A. Parlett, A. F. Lee, *Catal. Sci. Technol.* **2016**, *6*, 81.
[49] K. Mehrotra, G. S. Yablonsky, A. K. Ray, *Ind. Eng. Chem. Res* **2003**, *42*, 2273.
[50] Z. Zhao, J. Arentz, L. A. Pretzer, P. Limpornpipat, J. M. Clomburg, R. Gonzalez, N. M. Schweitzer, T. Wu, J. T. Miller, M. S. Wong, *Chem. Sci.* **2014**, *5*, 3715.
[51] M. Qureshi, K. Takanabe, *Chem. Mater.* **2017**, *29*, 158.

Residual Pd in organic semiconductor nanoparticles is essential for their photocatalytic activity. The cross coupling catalyst $Pd_2(dba)_3$ used in conjugated polymer synthesis decomposes to form Pd nanoparticles within the polymer. These act as a hydrogen evolution co-catalyst which enables electron transfer from the polymer to the surrounding aqueous protons.

The Effect of Residual Palladium Catalyst Contamination on the Photocatalytic Hydrogen Evolution Activity of Conjugated Polymers



Residual Pd in organic semiconductor nanoparticles is essential for their photocatalytic activity. The cross coupling catalyst $Pd_2(dba)_3$ used in conjugated polymer synthesis decomposes to form Pd nanoparticles within the polymer. These Pd nanoparticles act as a hydrogen evolution cocatalyst which enables electron transfer from the polymer to surrounding aqueous protons.

Copyright WILEY-VCH Verlag GmbH & Co. KGaA, 69469 Weinheim, Germany, 2016.